Geoderma 312 (2018) 36–44

Contents lists available at ScienceDirect

Geoderma

journal homepage: www.elsevier.com/locate/geoderma

Phytolith accumulation in broadleaf and conifer forests of northern China: Implications for phytolith carbon sequestration

Xiaomin Yang[a], Zhaoliang Song[a,*], Hongyan Liu[b], Lukas Van Zwieten[c], Alin Song[d], Zimin Li[e], Qian Hao[a], Xiaodong Zhang[a], Hailong Wang[f,g]

[a] Institute of the Surface-Earth System Science Research, Tianjin University, Tianjin 300072, China
[b] College of Urban and Environmental Sciences, Peking University, Beijing 100871, China
[c] New South Wales Department of Primary Industries, 1243 Bruxner Highway, Wollongbar, NSW 2477, Australia
[d] Institute of Agricultural Resources and Regional Planning of Chinese Academy of Agricultural Sciences, Beijing 100081, China
[e] Soil Science and Environment Geochemistry, Earth and Life Institute, Université catholique de Louvain, Croix du Sud 2/L7.05.10, 1348 Louvain-la-Neuve, Belgium
[f] School of Environment and Chemical Engineering, Foshan University, Foshan, Guangdong 528000, China
[g] Key Laboratory of Soil Contamination Bioremediation of Zhejiang Province, Zhejiang Agricultural and Forestry University, Lin'an, Hangzhou 311300, China

ARTICLE INFO

Keywords:
Biogenic silica
Long-term carbon sequestration
Phytolith occluded carbon
Soil organic carbon
Silicon-carbon coupled cycle
Temperate forest

ABSTRACT

Carbon (C) occlusion within phytoliths (PhytOC) has a significant potential for long-term C sequestration in forest ecosystems. To unravel the role of forest composition on phytolith production, soil phytolith distribution, and phytolith C sequestration in soils, we investigated community composition and examined phytoliths and PhytOC of mature leaves or needles of dominant trees and understory herbs, as well as soil profiles (50 cm depth) within *Quercus*, *Betula*, *Larix* and *Pinus* forest ecosystems of northern China. Results showed that herb layers contributed 72%, 52%, 40%, and 5% to the flux of phytolith production within *Betula* forest (18.0 ± 1.26 kg ha^{-1} yr^{-1}), *Quercus* forest (28.5 ± 0.77 kg ha^{-1} yr^{-1}), *Larix* forest (37.7 ± 1.80 kg ha^{-1} yr^{-1}) and *Pinus* forest (16.9 ± 0.30 kg ha^{-1} yr^{-1}), respectively. The distribution pattern of soil phytoliths from topsoil to subsoil could be classified into three types: significantly decreasing pattern (*Betula* forest and *Quercus* forest), non-significantly decreasing pattern (*Larix* forest), and initially increasing and then decreasing pattern (*Pinus* forest). Within 0–50 cm soil depth, the PhytOC storage of *Betula* forest, *Quercus* forest, *Larix* forest and *Pinus* forest were 0.29 ± 0.02 t ha^{-1}, 0.67 ± 0.03 t ha^{-1}, 0.46 ± 0.03 t ha^{-1} and 0.37 ± 0.02 t ha^{-1}, respectively. Moreover, the soil PhytOC turnover times of these four forest types were estimated to be 537,503,363 and 560 year, respectively, which were at least 8–20 times slower than soil organic carbon contributing to climate change mitigation. Overall, our findings indicate that composition of the forest community controls the production flux of phytoliths and the distribution of soil phytoliths, and influences the biogenic silica and its coupled carbon cycles.

1. Introduction

Forests store about 90% of all living terrestrial biomass carbon (C) on earth and afforestation/reforestation has been regarded as an effective solution to reduce atmospheric carbon dioxide (CO_2) (Christian, 2003). In China, national-scale projects including afforestation and reforestation have been launched in the past several decades (Fang et al., 2001; FAO, 2010). Although the estimated average CO_2 accumulation rate of Chinese forests is up to 110 t CO_2 ha^{-1} yr^{-1} (FAO, 2010), approximately 95% of the previously sequestered CO_2 will be released to atmosphere with only 5.5 t CO_2 ha^{-1} yr^{-1} captured by soil as organic C (Dewar and Cannell, 1992). The biogeochemical C sequestration by phytoliths provides a longer-term opportunity to sequester atmospheric CO_2 (Parr and Sullivan, 2005; Parr et al., 2010; Song et al., 2016).

Both understory herbs and tree leaves (or needles) in forest ecosystems play a crucial role in the biogeochemical silicon (Si) cycle and subsequent phytolith C sequestration (Zhang et al., 2012; Song et al., 2013), though underground fine roots may also contribute to soil Si content (Maguire et al., 2017). Generally, the leaves accumulate 50%–88% of the Si following root absorption of soil soluble Si (Chen et al., 1997; Carnelli et al., 2001; Feng et al., 1999; Umemura and Takenaka, 2014). In forest ecosystems, leaf litter could contribute between 28 and 87% of the total litter biomass (Chen et al., 1997; Carnelli

* Corresponding author at: Institute of the Surface-Earth System Science Research, Tianjin University, No. 92 Weijin Road Nankai District, Tianjin 300072, China.
E-mail address: zhaoliang.song@tju.edu.cn (Z. Song).

http://dx.doi.org/10.1016/j.geoderma.2017.10.005
Received 4 July 2017; Received in revised form 4 October 2017; Accepted 6 October 2017
Available online 13 October 2017

et al., 2001), meanwhile understory vegetation contributes approximately 28% of the annual net primary production (ANPP) (Chen et al., 1997; Feng et al., 1999; Song et al., 2013; Yang et al., 2015). Therefore, the understory herbs are also indispensable for the structure and function of forest ecosystems, especially for the nutrient cycling (e.g. nitrogen, Si and C) in forests ecosystems (Gilliam, 2007; Song et al., 2013).

Phytoliths are the main products of Si deposition inside cells and cell walls of plant bodies after plant absorption of the dissolved Si in the form of $Si(OH)_4$ or H_4SiO_4 from soil solution (Wilding, 1967; Epstein, 1994). Compared to lumen phytoliths, cell wall phytoliths generally contain less proteins, lipids and possibly nucleic acids (Hodson, 2016). The role of phytoliths in plants is diverse and multi-functional when the plants undergo adverse conditions (Epstein, 2009). For example, phytoliths can enhance the resistance against biotic and abiotic stress of many terrestrial plants, especially grasses (e.g. Cyperaceae and Poaceae) (Epstein, 2009). Furthermore, the morphology and chemical composition of phytoliths and environmental conditions would be expected to affect C sequestration in phytoliths (Song et al., 2016). In the plant kingdom, the phytolith content of plant dry weight varies greatly, being between 0.1% to > 10% (Epstein, 1994; Carnelli et al., 2001). For example, gymnosperms generally accumulate fewer phytoliths than angiosperms, and other monocots within the angiosperms commonly accumulate fewer phytoliths than Poaceae and Cyperaceae (Hodson et al., 2005; Yang et al., 2015). The annual biogenic Si production of terrestrial ecosystems has been estimated to be 60–200 Tmol Si yr^{-1}, equivalent to 3600–12,000 Tg yr^{-1} phytoliths, which may significantly influence global C cycle (Conley, 2002; Song et al., 2012).

As the most important component of terrestrial ecosystems, forest ecosystems not only play a crucial role in the biogenic Si cycle but can also effectively regulate atmospheric CO_2 concentration through the coupled biogeochemical cycles of Si and C (Chen et al., 1997; Meunier et al., 1999; Conley, 2002; Parr et al., 2010; Song et al., 2013). It has been confirmed that approximately 0.1–6% of organic C could be occluded within phytoliths (PhytOC, phytolith-occluded C) during the formation process of phytoliths (Jones and Milne, 1963; Parr and Sullivan, 2011; Zuo and Lü, 2011). During the decomposition of dead plants and annual litterfall, PhytOC will be released into soils or sediments (Bartoli, 1983). Compared with other soil organic C (SOC) fractions, PhytOC is more stable and can be kept in soils for thousands of years under the protection of silica (Piperno, 1985; Strömberg, 2004; Parr and Sullivan, 2005; Zuo et al., 2017). Furthermore, soil PhytOC can contribute to 15–37% of the average annual accumulation rate of the global stable soil C (88 kg CO_2 ha^{-1} yr^{-1}) and can account for 82% of the total C in some about 2000 year-old soils (Parr and Sullivan, 2005). For phytolith C sequestration, past researches mainly focused on sugarcane (Parr et al., 2009), bamboo (Parr et al., 2010), millet (Zuo and Lü, 2011), wheat (Parr and Sullivan, 2011) and rice (Li et al., 2013), and their PhytOC production fluxes significantly ranged from 0.04 to 0.71 t CO_2 ha^{-1} yr^{-1}. Despite great advances in estimating production fluxes of PhytOC for some terrestrial ecosystems (e.g. grasslands, wetlands, and croplands) (Song et al., 2012; Li et al., 2013; Song et al., 2014), few studies have focused on the effects of the community compositions on the production fluxes, distributions and storage processes of phytoliths and PhytOC in forest ecosystems.

In this study, we hypothesized that: i) forest composition controls the quantity and characteristics of above-ground phytoliths; ii) the stability and distribution of under-ground phytoliths are related to forest composition; iii) being protected by phytoliths, the decomposition of soil PhytOC is significantly slower than SOC. These factors are important for the long-term sequestration of C in soils. In order to test our hypotheses, we examined the effects of forest composition on phytolith and PhytOC production fluxes and phytolith distribution in soils, and estimated the long-term phytolith C sequestration potential of *Betula*, *Quercus*, *Larix*, and *Pinus* forest ecosystems in northern China. Our study will offer scientific reference for the global long-term C sequestration practices such as afforestation and reforestation.

2. Materials and methods

2.1. Experimental site

This study was carried out in the mountain area of Northern Hebei (42°09′–42°26′N, 117°09′–117°26′E), China. The experimental area belongs to continental semi-arid sub humid climate with mean annual temperature (MAT) of 0–13 °C and mean annual precipitation (MAP) of 300–800 mm (Yang et al., 2015). The altitude of this area is between 1000 and 1940 m. There are four typical temperate forests in this area: *Betula* forest (dominated by *Betula platyphylla* and *Betula davurica*), *Quercus* forest (dominated by *Quercus mongolica*), *Larix* forest (dominated by *Larix principis-rupprechtii*), and *Pinus* forest (dominated by *Pinus tabulaeformis*). The soils of this area are composed of Haplic Kastanozem according to the Food and Agriculture Organization (FAO) soil classification system (IUSS Working Group WRB, 2015).

2.2. Field investigation and sampling

In the field investigations, we randomly set three 1 m × 1 m quadrats for understory herb layer and 10 m × 10 m quadrats for tree layer as standard plots in each forest type in July 2012. The vegetation information, such as height, abundance, and cover of each plant species, were recorded in each plot (Appendix A). Plant species nomenclature was based on *Flora of China* (http://www.eflora.cn).

Considering that the main production of phytoliths occurs in mature tree leaves (or needles) and above-ground herbs in terrestrial forest ecosystems (Bartoli, 1983; Carnelli et al., 2001; Hodson et al., 2005; Umemura and Takenaka, 2014), this study selected mature leaves (or needles) and above-ground herbs to examine phytolith and PhytOC content. For the tree layer, mature leaves of *Betula platyphylla*, *Betula davurica* and *Quercus mongolica*, mature needles of *Larix principis-rupprechtii*, and mature needles (> two years old) of *Pinus tabulaeformis* in corresponding forest type were sampled from each standard plot (Table 1). For understory herbs, twelve of thirty-two, nine of twenty-seven, eight of twenty-seven, and five of seven dominant plant species in the herb layer in *Betula*, *Quercus*, *Larix*, and *Pinus* forest were also sampled, respectively (Table 1). Each plant sample included approximately 150 g.

Furthermore, soil samples were sampled by soil auger in each forest type. In order to minimize the spatial heterogeneity in soil conditions, we randomly selected three soil sample sites in each forest type. In each site, soil samples (about 500 g) were collected from the layers of 0–10 cm, 10–20 cm, 20–30 cm, 30–40 cm, and 40–50 cm. Additionally, characteristics (e.g. earthworm channels and earthworms) of each soil layer were also recorded.

2.3. Sample analysis

Plant samples were placed in an ultrasonic bath for 15 min, rinsed three times with ultrapure water, dried at 75 °C for 48 h to a constant mass, and then ground to a coarse and fine powder. Soil samples were dried by air, ground by a mortar and pestle, and then respectively sieved to 10 mesh (2 mm pore size), 40 mesh (0.43 mm pore size) and 100 mesh (0.15 mm pore size).

According to the study of Tian et al. (2011), conversion factors of 0.48, 0.49, 0.44 and 0.54 between biomass and organic C were used to estimate foliage organic C content of *Betula*, *Quercus*, *Larix* and *Pinus* forests, respectively. Moreover, the conversion factor of 0.45 between biomass of herbs and organic C has frequently been used to estimate organic C content of the herbs (Vogt, 1991). To examine total content of plant Si, the fine powder samples of plants were fused by Li-metaborate and dissolved in dilute nitric acid (4%); the Si concentration of the solution was analyzed by molybdenum blue colorimetric method (Lu,

Table 1
SiO_2 content, Phytolith content, C in phytoliths, PhytOC content, and important value (IV) of different species in the studied forest communities.

Forest type	Species	SiO_2 in biomass (g kg^{-1})[a]	Phytoliths in biomass (g kg^{-1})[a]	C in phytoliths (g kg^{-1})[a]	PhytOC in biomass (g kg^{-1})[a]	IV (%)[b]
Betula	Herb layer					
	Saussurea ussuriensis	8.48 (1.86)	6.92 (1.42)	16.6 (1.54)	0.104 (0.039)	8.98
	Carex lanceolata	29.0 (0.32)	28.2 (1.49)	25.4 (2.13)	0.658 (0.094)	9.62
	Sanguisorba officinalis	11.1 (0.43)	5.61 (3.57)	20.0 (2.36)	0.125 (0.095)	4.58
	Paeonia lactiflora	0.88 (0.19)	0.71 (0.14)	17.4 (2.00)	0.014 (0.007)	2.56
	Geranium eriostemon	3.30 (0.11)	2.43 (0.29)	15.3 (0.87)	0.035 (0.030)	3.74
	Vicia pseudo-orobus	0.94 (0.01)	0.75 (0.00)	19.7 (4.30)	0.018 (0.000)	3.82
	Vicia unijuga	4.68 (0.18)	3.74 (0.14)	20.4 (3.64)	0.090 (0.003)	3.65
	Thalictrum petaloideum	4.12 (0.22)	3.29 (0.17)	20.3 (3.74)	0.079 (0.004)	1.64
	Polygonum viviparum	1.38 (0.11)	1.10 (0.08)	19.8 (4.22)	0.026 (0.002)	3.85
	Valeriana officinalis	4.31 (0.43)	3.45 (0.34)	20.3 (3.70)	0.083 (0.008)	3.57
	Patrinia scabiosaefolia	4.97 (0.22)	2.93 (0.18)	18.4 (2.04)	0.060 (0.005)	2.80
	Campanula punctata	11.0 (0.54)	10.2 (1.08)	15.4 (4.25)	0.114 (0.020)	2.42
	Tree layer					
	Betula platyphylla	1.10 (0.03)	0.98 (0.03)	15.4 (0.06)	0.015 (0.001)	94.9
	Betula davurica	1.76 (0.05)	1.64 (0.30)	15.2 (0.58)	0.024 (0.002)	5.14
Quercus	Herb layer					
	Carex lanceolata	15.6 (0.02)	13.6 (1.16)	20.7 (0.37)	0.278 (0.051)	25.2
	Clematis hexapetala	7.59 (1.07)	4.67 (0.13)	16.4 (0.75)	0.073 (0.008)	2.63
	Poa sphondylodes	20.1 (0.21)	16.7 (0.05)	31.5 (9.01)	0.674 (0.170)	2.61
	Sanguisorba officinalis	11.4 (1.63)	9.12 (1.31)	21.6 (2.45)	0.219 (0.031)	2.69
	Spodiopogon sibiricus	27.0 (11.0)	21.6 (8.77)	24.3 (0.31)	0.517 (0.210)	3.56
	Hemerocallis minor	5.68 (0.11)	4.54 (0.09)	20.5 (3.46)	0.109 (0.002)	4.51
	Adenophora tetraphylla	6.56 (5.19)	14.1 (0.63)	21.6 (0.27)	0.307 (0.016)	3.64
	Indigofera bungeana	1.17 (0.07)	0.94 (0.06)	19.7 (4.26)	0.022 (0.001)	3.18
	Iris ruthenicar	13.1 (0.10)	8.13 (2.43)	17.0 (1.65)	0.125 (0.037)	3.22
	Tree layer					
	Quercus mongolica	5.63 (0.08)	4.05 (0.21)	54.4 (37.5)	0.372 (0.078)	100
Larix	Herb layer					
	Carex lanceolata	35.5 (1.07)	26.1 (1.53)	24.6 (2.01)	0.589 (0.164)	12.5
	Agrimonia pilosa	1.17 (0.09)	0.93 (0.07)	19.7 (4.26)	0.022 (0.002)	2.45
	Vicia unijuga	1.71 (0.11)	1.48 (0.02)	15.4 (0.36)	0.022 (0.013)	3.09
	Epilobium angustifolium	0.82 (0.04)	0.65 (0.03)	19.7 (4.32)	0.016 (0.001)	18.4
	Artemisia argyi	7.16 (0.02)	4.95 (0.75)	17.4 (0.17)	0.087 (0.015)	6.34
	Tephroseris kirilowii	9.49 (0.22)	6.43 (1.34)	15.4 (2.52)	0.083 (0.017)	2.81
	Taraxacum mongolicum	6.92 (0.11)	4.01 (1.61)	20.1 (3.21)	0.093 (0.042)	0.96
	Bromus inermis	20.6 (0.53)	25.4 (2.35)	28.5 (2.15)	0.776 (0.133)	4.50
	Tree layer					
	Larix principis-rupprechtii	8.96 (0.38)	6.48 (0.04)	36.6 (18.6)	0.357 (0.084)	100
Pinus	Herb layer					
	Carex lanceolata	29.0 (1.00)	24.1 (1.50)	20.5 (5.21)	0.369 (0.200)	27.9
	Artemisia eriopoda	0.89 (0.03)	0.71 (0.03)	19.7 (4.31)	0.017 (0.001)	19.3
	Asparagus cochinchinensis	8.96 (5.06)	7.16 (4.05)	21.1 (2.88)	0.172 (0.097)	9.66
	Lespedeza bicolor	5.47 (1.48)	4.37 (1.18)	20.5 (3.50)	0.105 (0.028)	7.68
	Artemisia sacrorum	6.98 (2.75)	5.58 (2.20)	20.8 (3.23)	0.134 (0.053)	17.3
	Tree layer					
	Pinus tabulaeformis	7.01 (0.21)	7.29 (0.13)	33.7 (15.4)	0.358 (0.019)	100

[a] Data present as means with standard deviation (in brackets).
[b] More details see Appendix A.

2000). Phytoliths from the plant coarse samples were extracted using microwave digestion as described by Parr and Sullivan (2014). Phytoliths from soil samples (40 mesh) were isolated using a heavy liquid suspension after microwave digestion (Li et al., 2013; Zuo et al., 2014). To ensure that all extraneous organic materials outside of the phytoliths were thoroughly removed, the extracted phytoliths were cleaned up using a Walkley-Black method (Walkley and Black, 1934). These phytoliths were oven-dried at 65 °C for 24 h in a centrifuge tube and then weighed to obtain the content after cooling. We used the classical potassium dichromate method to determine PhytOC content whereby PhytOC was released from phytoliths after HF (1 mol/L) digestion (Lu, 2000; Li et al., 2013). In addition, the 100 mesh soil samples was used to determine soil organic carbon (SOC) using the method of classical potassium dichromate (Walkley and Black, 1934), and the 10 mesh soil samples was used to analyze soil pH with a pH meter (PB-10, Sartorius, Germany) in a 1: 2.5 soil: water suspension (Lu, 2000). Quality assurance for the analysis of Si, SOC and PhytOC was monitored using standard soil samples (GBW07405) with a precision of 7% obtained (Li et al., 2013).

2.4. Data analysis

The importance value (IV) was regarded as a weight of each plant species when estimating the comprehensive index of communities (ter Braak, 1986; Qiu et al., 2016). In each standard plot, the IV (%) of each species was calculated by:

$$IV = (RH + RC + RA)/3 \quad (1)$$

in which RH (%) is referred to the relative height of each species, RC (%) is referred to the relative cover of each species, and RA (%) is referred to the relative abundance of each species (Liu et al., 2008).

In each standard plot, the weighted mean (WM) of a given functional trait for each species was calculated by:

$$WM_i = IV_i \times X_i \quad (2)$$

in which WM_i (g kg^{-1}) is the weighted mean of the measured functional trait for species *i*, IV_i is the importance value of species *i* and can be calculated from Formula (1), X_i (g kg^{-1}) is the content of the measured functional trait for each species *i*.

Community weighted mean (CWM) as an integrative calculation

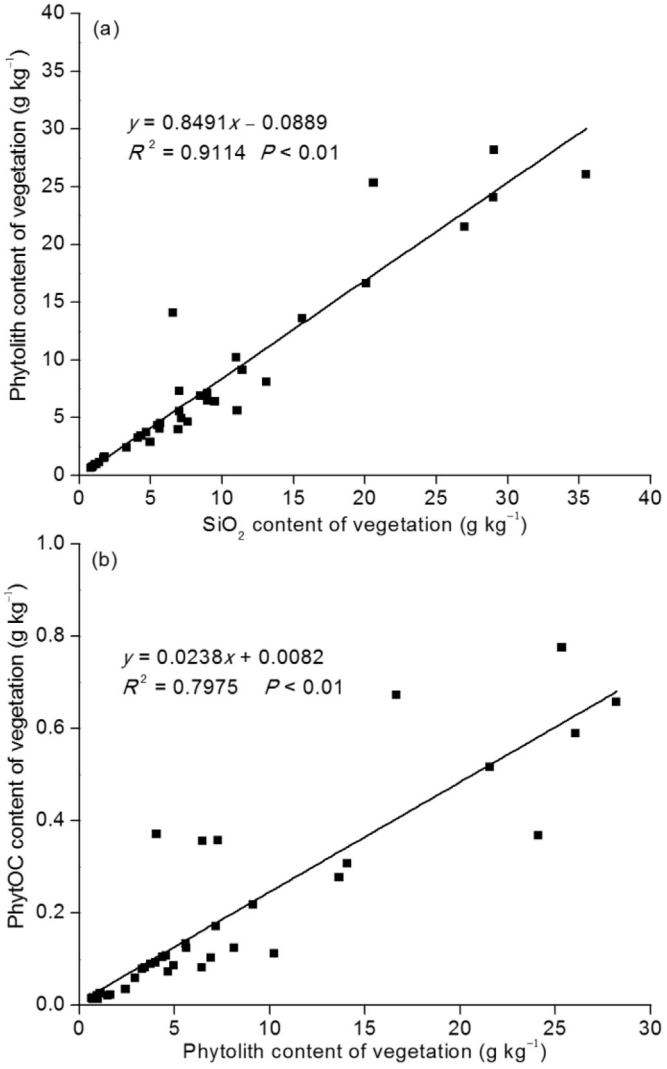

Fig. 1. Correlation between phytolith content and SiO_2 content (a) and between PhytOC content and phytolith content (b) in aboveground vegetation.

method is broadly used to explain and assess the distribution patterns of some community functional traits by many researchers (Ricotta and Moretti, 2011; Qiu et al., 2016). In order to assess the CWM of different measured functional traits more comprehensively and persuasively, this study calculated the CWM of different measured functional traits in each standard plot as:

$$CWM = \sum_{i=1}^{s} WM_i / IV_{total} \quad (3)$$

where WM_i (g kg^{-1}) is referred to as the weighted mean of the measured functional trait for species i and can be calculated from Formula (2), S is the total number of sampled species, IV_{total} is the sum total of importance values of all sampled species, and CWM (g kg^{-1}) is the community weighted mean of the measured functional trait.

In order to assess the effects of community composition on the production fluxes (PF) of different measured functional traits in different forest above-ground components, the estimation was modified from Song et al. (2012 and 2013) as:

$$PF = ANPP \times CWM \quad (4)$$

where PF (kg ha^{-1} yr^{-1}) is the production flux of the measured functional trait of each forest above-ground component, ANPP (t ha^{-1} yr^{-1}) is the annual net primary productivity of herbs and tree leaves in each forest, CWM (g kg^{-1}) is the community weighted mean of the measured functional trait and can be calculated from Formula (3).

The storage (ST) of a given functional trait in soil was calculated by:

$$ST = \sum_{i=1}^{n} T_i \times BD_i \times X_i \quad (5)$$

where ST (t ha^{-1}) is the storage of the measured functional trait in soil, i (i = 1, 2, 3, 4, 5) stands for the soil profile layer from topsoil to subsoil (i.e., 0–10, 10–20, 20–30, 30–40, and 40–50 cm), T_i (cm) is the thickness of the soil layer i, BD_i (g cm^{-3}) is the bulk density of the soil layer i, and X_i (g kg^{-1}) is the content of the measured functional trait in soil layer i.

Assuming that the turnover of the measured functional traits in soils achieved a dynamic balance, the turnover time (TT) of the measured functional traits was estimated as:

$$TT = ST/PF \quad (6)$$

where TT (year) is the turnover time of the measured functional trait in soils, ST (t ha^{-1}) is the storage of the measured functional trait in soils and can be calculated from Formula (5), and PF (t ha^{-1} yr^{-1}) is the production flux of the measured functional trait in different forest above-ground parts and can be calculated from Formula (4).

2.5. Data statistics

The data presented in this study are the average of three replicates. Excel and SPSS (18.0) were used to statistically analyze the data. Normal distribution of the data was tested by Shapiro-Wilk test. One-way analysis of variance (ANOVA) and the least significant difference (LSD) test were applied to examine the differences between the data groups. Figures were made with Origin (8.0).

3. Results

3.1. Ecological measurements of phytogenic SiO_2, phytoliths and PhytOC

For 34 dominant plant species of the herb layer, the total SiO_2 and phytolith content of above-ground biomass varied from 0.82 to 29.0 g kg^{-1} and 0.65 to 28.2 g kg^{-1}, respectively; the C content of phytoliths was 15.3–31.5 g kg^{-1}; and the PhytOC content of above-ground biomass was 0.014–0.776 g kg^{-1} (Table 1). For 5 dominant tree species, the total SiO_2 and phytolith content of mature leaves (or needles) varied from 1.10 to 8.96 g kg^{-1} and 0.98 to 7.29 g kg^{-1}, respectively; the C content of phytoliths was 15.2–54.4 g kg^{-1}; and the PhytOC content of mature leaves (or needles) was 0.015–0.372 g kg^{-1} (Table 1). Additionally, the correlations between SiO_2 content and phytolith content (R^2 = 0.9114, P < 0.01) and between phytolith content and PhytOC content (R^2 = 0.7975, P < 0.01) in the 39 sampled species were strongly positive (Fig. 1).

As shown in Table 2, both the community weighted mean of phytolith (CMW-phytolith) and community weighted mean of PhytOC (CMW-PhytOC) in herbs were higher than those in mature leaves (or needles) for each forest. For herbs, the variations of both CWM-phytolith content (8.62–10.8 g kg^{-1}) and CMW-PhytOC content (0.18–0.24 g kg^{-1}) among different forests were similar. For mature leaves (or needles), the highest CMW-phytolith and CMW-PhytOC were found in *Pinus* forest (7.29 g kg^{-1} and 0.17 g kg^{-1}, respectively). The CMW-phytolith and CMW-PhytOC of litters, including herbs, varied from 9.63 to 18.1 g kg^{-1} and 0.20 to 0.36 g kg^{-1}, respectively, among different forests. In addition, the variations of CWM-PhytOC in litters, which mainly comprised of herb layers and mature leaves (or needles) of dominant trees, were analogous to the variations of CWM-phytolith (Table 2).

Organic C production flux comprised of tree foliage and herb in *Betula*, *Quercus*, *Larix* and *Pinus* forests was estimated to be 3.02, 2.34,

Table 2
The measured functional traits of aboveground vegetation.

Forest type	ANPP (t ha^{-1} year^{-1})[a]	CWM-Phytolith (g kg^{-1})[b]	CWM-PhytOC (g kg^{-1})[b]	Organic C production flux (t ha^{-1} yr^{-1})[c]	Phytolith production flux (kg ha^{-1} yr^{-1})[b]	PhytOC production flux (kg ha^{-1} yr^{-1})[b]
Herb						
Betula	1.51	8.62 (0.66)	0.18 (0.02)	0.68	13.0 (0.99)	0.28 (0.03)
Quercus	1.51	9.77 (0.03)	0.22 (0.07)	0.68	14.7 (0.05)	0.34 (0.10)
Larix	1.49	10.0 (1.12)	0.24 (0.08)	0.67	15.0 (1.67)	0.36 (0.12)
Pinus	0.08	10.8 (0.19)	0.19 (0.01)	0.04	0.87 (0.02)	0.02 (0.00)
Mature leaf						
Betula	4.88	1.01 (0.06)	0.02 (0.00)	2.34	4.92 (0.27)	0.08 (0.01)
Quercus	3.41	4.05 (0.21)	0.03 (0.01)	1.67	13.8 (0.73)	0.51 (0.04)
Larix	3.51	6.48 (0.04)	0.12 (0.00)	1.54	22.7 (0.12)	0.42 (0.01)
Pinus	2.19	7.29 (0.13)	0.17 (0.01)	1.18	16.0 (0.28)	0.37 (0.03)
Litters (Herb + Mature leaf)						
Betula	6.39	9.63 (0.71)	0.20 (0.02)	3.02	18.0 (1.26)	0.35 (0.03)
Quercus	4.92	13.8 (0.24)	0.26 (0.08)	2.35	28.5 (0.77)	0.85 (0.14)
Larix	5.00	16.5 (1.16)	0.36 (0.08)	2.21	37.7 (1.80)	0.77 (0.13)
Pinus	2.27	18.1 (0.31)	0.36 (0.02)	1.22	16.9 (0.30)	0.39 (0.03)

[a] The ANPP data of herb and litter are from Chen et al. (1997) and Feng et al. (1999).
[b] Data present as means with standard deviation (in brackets).
[c] More details see Materials and methods.

2.21 and 1.22 t ha^{-1} yr^{-1}, respectively (Table 2). Combining the published ANPP data with measured CMW-phytolith of herbs and mature leaves (or needles) in each forest, we also estimated the phytolith production flux of the forests (Table 2). For herbs, the high phytolith production flux was found in *Larix* forest (15.0 kg ha^{-1} yr^{-1}). For mature leaves, the high phytolith production flux was also found in *Larix* forest (22.7 kg ha^{-1} yr^{-1}). Therefore, the phytolith production flux of litters in *Larix* forest (37.7 kg ha^{-1} yr^{-1}) was higher than that in *Quercus* forest (28.5 kg ha^{-1} yr^{-1}), *Betula* forest (18.0 kg ha^{-1} yr^{-1}) and *Pinus* forest (16.9 kg ha^{-1} yr^{-1}) (Table 2). Similarly, the PhytOC production flux of litters in each forest could be also estimated and varied from 0.35 to 0.85 kg ha^{-1} yr^{-1} (Table 2).

3.2. Variations of the measured functional traits in different forest soil profiles

Soil pH in the 0–50 cm soil layers of *Betula*, *Quercus*, *Larix*, and *Pinus* forests ranged from 6.34 to 6.62, 6.99 to 7.44, 6.06 to 6.91, and 5.82 to 6.68, respectively (Table 3), with the *Pinus* forest being the most acidic. SOC contents in 0–50 cm soil profiles decreased from topsoil to the subsoil in all forests (Table 3). The distribution pattern of soil phytoliths from topsoil (0–10 cm) to subsoil (40–50 cm) could be classified into three types: significantly decreasing pattern (Fig. 2a, b), non-significantly decreasing pattern (Fig. 2c), and initially increasing and then decreasing trend (Fig. 2d). For details, the phytolith contents in the soil layers (0–50 cm) of *Betula* forest, *Quercus* forest, *Larix* forest, and *Pinus* forest varied from 3.40 to 9.13 g kg^{-1}, 2.94 to 7.13 g kg^{-1}, 3.24 to 4.31 g kg^{-1}, and 2.69 to 7.02 g kg^{-1}, respectively (Fig. 2). Within the 0–50 cm soil layers (Table 3), the C in phytoliths was 5.87 to 16.0 g kg^{-1}; although the PhytOC content only ranged from 0.027 to 0.086 g kg^{-1}, the contribution of PhytOC to total SOC significantly increased from topsoil to the subsoil (Fig. 3).

Furthermore, our results showed that the SOC storage of *Betula*, *Quercus*, *Larix* and *Pinus* forests (0–50 cm soil depth) were 131, 59.2, 104 and 89.9 t ha^{-1}, respectively, whereas the soil PhytOC storage of these four forests (0–50 cm soil depth) were only 0.29, 0.67, 0.46 and 0.37 t ha^{-1}, respectively (Fig. 4a). Assuming the SOC was from tree foliage and herb only, the turnover time of SOC in *Betula*, *Quercus*, *Larix*

Table 3
The soil bulk density (BD), pH, organic carbon (SOC), carbon (C) in phytoliths and PhytOC content within 0–50 cm soil depth of the studied forests.

Forest type	Soil depth (cm)	Soil BD (g cm^{-3})[a]	Soil pH[b]	SOC (g kg^{-1})[b]	C in phytoliths (g kg^{-1})[b]	PhytOC content (g kg^{-1})[b]
Betula	0–10	0.94	6.62 (0.03)	43.4 (0.14)	6.48 (0.10)	0.059 (0.002)
	10–20	1.00	6.34 (0.01)	27.1 (0.16)	6.54 (0.16)	0.035 (0.000)
	20–30	1.02	6.44 (0.08)	22.2 (0.14)	8.54 (1.01)	0.032 (0.005)
	30–40	1.05	6.57 (0.09)	19.0 (0.59)	6.82 (0.73)	0.027 (0.002)
	40–50	1.06	6.45 (0.06)	19.1 (0.40)	11.8 (6.03)	0.036 (0.004)
Quercus	0–10	0.95	6.99 (0.06)	13.4 (0.02)	12.1 (0.14)	0.086 (0.005)
	10–20	1.20	7.16 (0.03)	12.5 (0.72)	14.5 (1.54)	0.085 (0.003)
	20–30	1.25	7.24 (0.04)	11.1 (0.05)	13.2 (2.37)	0.081 (0.003)
	30–40	1.28	7.38 (0.04)	8.64 (0.07)	13.9 (1.84)	0.065 (0.008)
	40–50	1.26	7.44 (0.06)	5.23 (0.10)	16.0 (3.00)	0.047 (0.004)
Larix	0–10	1.09	6.06 (0.12)	23.5 (1.08)	9.79 (2.71)	0.042 (0.009)
	10–20	1.23	6.82(0.05)	17.9 (0.42)	11.4 (2.78)	0.049 (0.023)
	20–30	1.25	6.83(0.01)	17.4 (0.90)	13.4 (0.51)	0.049 (0.002)
	30–40	1.28	6.89 (0.03)	15.1 (0.15)	12.4 (1.03)	0.045 (0.001)
	40–50	1.30	6.91 (0.01)	12.1 (0.77)	13.2 (0.12)	0.043 (0.002)
Pinus	0–10	1.03	6.12 (0.04)	20.1 (0.51)	11.0 (1.00)	0.029 (0.003)
	10–20	1.09	6.68 (0.01)	15.8 (0.54)	9.56 (0.68)	0.031 (0.006)
	20–30	1.15	6.45 (0.05)	15.8 (0.01)	9.30 (0.43)	0.056 (0.003)
	30–40	1.17	5.66 (0.03)	15.6 (0.85)	6.91 (0.41)	0.049 (0.003)
	40–50	1.17	5.82 (0.03)	13.4 (1.12)	5.87 (0.88)	0.027 (0.000)

[a] The soil BD data are based on Zhang et al. (2011), Liu et al. (2012) and Zhao et al. (2013), which are located close to our study areas.
[b] Data present as means with standard deviation (in brackets).

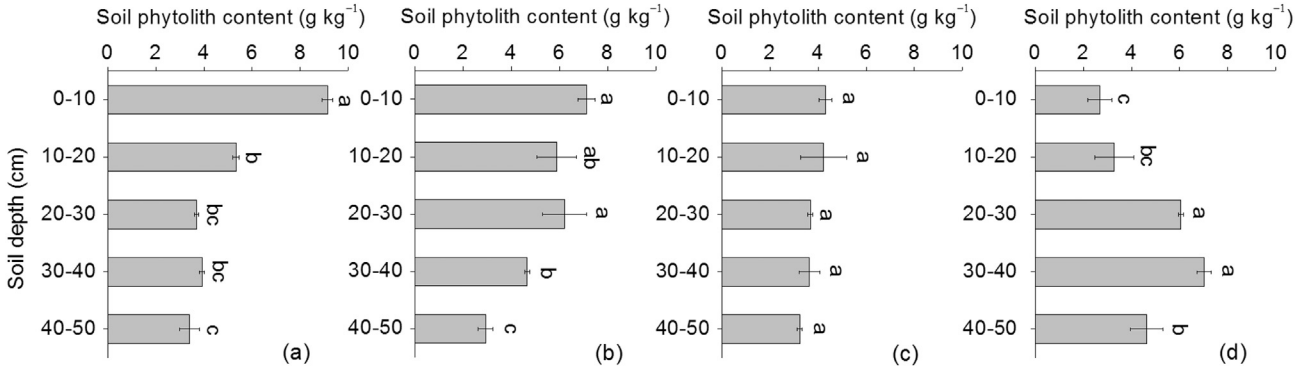

Fig. 2. Phytolith variation from topsoil to subsoil in *Betula* forest (a), *Quercus* forest (b), *Larix* forest (c), and *Pinus* forest (d). Different lowercase letters indicate significant differences among the stands of soil depth at $P < 0.05$ level based on the least significant difference (LSD) test.

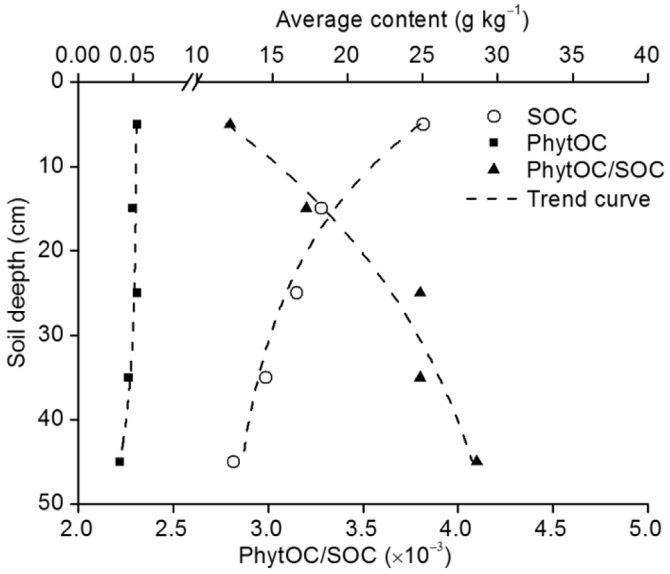

Fig. 3. Variation tendency of soil organic carbon (SOC) content, soil PhytOC content, and PhytOC/SOC in different soil layers. The values are the average mean of *Betula* forest, *Quercus* forest, *Larix* forest, and *Pinus* forest. The trend curve was obtained using the model $y = 17.53 \times e^{\frac{-x}{17.88}} + 4.48$ ($R^2 = 0.96$) for SOC, $y = -1.92 \times e^{\frac{x}{10.23}} + 0.05$ ($R^2 = 0.78$) for PhytOC, and $y = -2.03 \times e^{\frac{-x}{27.78}} + 4.48$ ($R^2 = 0.92$) for PhytOC/SOC.

and *Pinus* forests (0–50 cm soil depth) were estimated to be 43, 25, 47 and 71 years, respectively (Fig. 4b). By contrast, the turnover time of PhytOC in these four forests (0–50 cm soil depth) could reach up to 537, 503, 363 and 560 years, respectively (Fig. 4b).

4. Discussion

4.1. Effects of forest compositions on phytolith production

As the endpoint of the transpiration stream, the leaves (or needles) of herbs and trees are the main locations for accumulating SiO_2 in terrestrial ecosystems (Bartoli, 1983; Hodson et al., 2005; Cornelis et al., 2010; Umemura and Takenaka, 2014). The study of Cornelis et al. (2010) showed that the different SiO_2 contents of leaves (or needles) in *Pseudotsuga menziesii* (11.3 g kg^{-1}), *Picea abies* (9.7 g kg^{-1}), *Pinus nigra* (0.5 g kg^{-1}), *Fagus sylvatica* (15.9 g kg^{-1}), and *Quercus sessiliflora* (11.7 g kg^{-1}), which were sampled from same soil and climate conditions, were mainly controlled by tree species. In present study, the different SiO_2 contents of leaves (or needles) were also driven by tree species, including *Betula platyphylla* (1.10 g kg^{-1}), *Betula davurica* (1.76 g kg^{-1}), *Quercus mongolica* (5.63 g kg^{-1}), *Larix principis-rupprechtii* (8.96 g kg^{-1}), and *Pinus tabulaeformis* (7.01 g kg^{-1}) (Table 1).

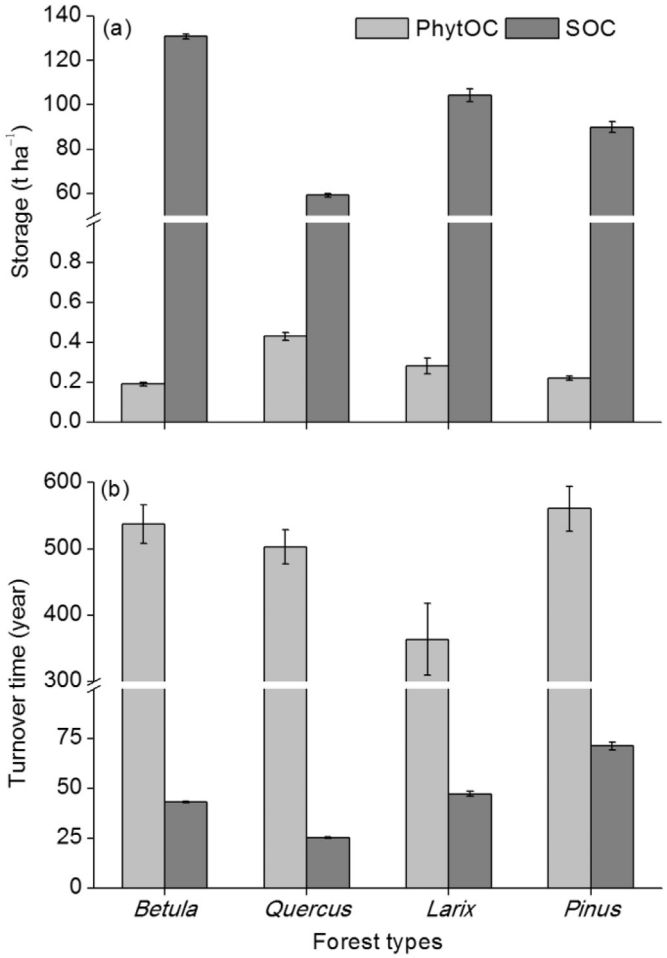

Fig. 4. Storage (a) and turnover time (b) of soil PhytOC and soil organic carbon (SOC) in each forest.

The significant correlation ($P < 0.01$) between total SiO_2 content and phytolith content in herbs and tree leaves (or needles) indicates that > 80% of the total SiO_2 can be accumulated into phytoliths (Fig. 1a). Generally, forest litters are derived mainly from herbs and tree leaves (or needles) (Chen et al., 1997; Feng et al., 1999). Therefore, the contents of phytoliths immobilized in herbs and tree leaves (or needles) and the biomass ratio of herbs and tree leaves (or needles) might affect the variation of phytolith content in litters for each forest. In present study (Table 2), the higher CWM-phytolith of combined litters in coniferous forests (*Larix* forest, 16.5 g kg^{-1}; *Pinus* forest, 18.1 g kg^{-1}) compared to those in broadleaf forests (*Betula* forest,

9.63 g kg^{-1}; *Quercus* forest, 13.8 g kg^{-1}) was mainly due to the CWM-phytolith content in mature needles of *Pinus tabulaeformis* (7.29 g kg^{-1}) and *Larix principis-rupprechtii* (6.48 g kg^{-1}) were higher than those in mature leaves of *Quercus mongolica* (4.05 g kg^{-1}), *Betula platyphylla* (0.93 g kg^{-1}) and *Betula davurica* (0.08 g kg^{-1}).

Previous studies have reported that ANPP can significantly control phytolith production fluxes (Blecker et al., 2006; Song et al., 2013). Among different forests, in spite of higher CWM-phytolith in herb layers, the ANPP of herb layers were lower than those of tree leaves or needles (Table 2). In order to investigate the importance of ecological communities for phytolith production, this study estimated the phytolith production fluxes in different forest ecosystems based on the community composition and structure of above-ground vegetation. As Table 2 showed, the herb layers and tree leaf layers respectively contributed 72% and 28% to the estimates of phytolith production fluxes in *Betula* forest (18.0 kg ha^{-1} yr^{-1}). For *Quercus* forest, the contributions of herbs (52%) and mature leaves (48%) to total phytolith production fluxes (28.5 kg ha^{-1} yr^{-1}) was nearly equivalent (Table 2). For the coniferous forests, the phytolith annual production fluxes of *Larix* forest (37.7 kg ha^{-1} yr^{-1}) comprised a 40% contribution from herb layers and 60% from tree leaf layers (Table 2). In stark contrast to the other forests, *Pinus* forest (16.9 kg ha^{-1} yr^{-1}) comprised a contribution of only 5% from herb layers and 95% from tree leaf layers (Table 2), which might be due to the high competitiveness of evergreen needles for light and the suppression of the herb layer by the accumulation of needles.

The phytolith content of each plant species is controlled mainly by phylogenetic factors (Hodson et al., 2005; Zhang et al., 2012; Yang et al., 2015), though other environmental effects such as topography, latitude, temperature, water availability, and Si availability in soils can also influence the phytolith production (Rosen and Weiner, 1994; Zhang et al., 2012; Yang et al., 2016). However, for ecological communities, our results indicate that the phytolith production fluxes are not only controlled by the phylogenetic level of plant species, but also by the composition and distribution of herbs and trees in different forests.

4.2. Effects of forest composition on soil phytolith distribution

Generally, the dissolution of phytoliths is still occurring during migration from topsoil to subsoil (Bartoli, 1983; Colin et al., 1992). Fraysse et al. (2009) suggest that the plant phytolith dissolution rates are increased when solution pH increased from 4 to 10. However, in deciduous broadleaf forest the variation of soil pH (Table 3) in each soil layer was minor (varied from 6.34 to 6.62 in *Betula* forest and from 6.99 to 7.44 in *Quercus* forest, respectively). In *Larix* forest soil pH increased slightly from topsoil (6.06) to subsoil (6.91). The relatively similar soil pH with depth suggests that soil pH is not an important factor on phytolith dissolution in this current study. Moreover, compared to plant phytoliths, soil phytoliths are less soluble due to the decreased availability of water, lower surface area and greater Al concentration of most soil phytoliths (Bartoli and Wilding, 1980; Li et al., 2014). Tree species can influence soil phytolith stability due to the variation in chemical characteristics of the phytoliths (Bartoli and Wilding, 1980; Bartoli, 1983, 1985; Blecker et al., 2006). For example, the biological cycle of Si in leaves (11.0–17.8 kg Si ha^{-1} yr^{-1}) is faster than that of needles (2.1–10.3 kg Si ha^{-1} yr^{-1}) in temperate deciduous and coniferous forests (Bartoli, 1983). Thus, the leaf phytoliths are more labile than needle phytoliths in temperate forest soils (Bartoli, 1983). The studies of Blecker et al. (2006) and Pan et al. (2017) reported that the soil phytoliths of different grasslands can exist in soils at a centennial-millennial scale, indicating that a majority of herb phytoliths are relatively stable.

In common with the translocation of synthetic particles, protozoan pathogens and bacteria in soils, the migration of phytoliths can be affected by their size and shape (Smith et al., 1985; van Elsas et al., 1991; Mawdsley et al., 1996; Burkhardt et al., 2008; Fishkis et al., 2010). Generally, small phytoliths (largest axis length < 7.5 μm or circle equivalent diameter < 6.25 μm) increase with soil depth, whereas the larger phytoliths (largest axis length > 17.5 μm or circle equivalent diameter < 11.25 μm) decrease with soil depth (Fishkis et al., 2010). Moreover, the fractions of "isometric" phytoliths (aspect ratio < 2) usually decrease with soil depth (Fishkis et al., 2010). In contrast, the "stretched" phytoliths (aspect ratio > 3) tend to increase with soil depth (Fishkis et al., 2010). *Larix* and *Pinus* needles tend to have small and stretched phytoliths (Wang and Lü, 1993), suggesting that they are more likely to increase with soil depth. However, the fractions of "isometric" and "large" phytoliths are usually accumulated in broadleaf tree leaves and herbs, especially in poaceae and cyperaceae (Wang and Lü, 1993). For example, Meunier et al. (2017) showed that most phytoliths in *Triticum turgidum*, as well as most grasses, are crenate and rondel morphotypes (20–100 μm long) from silica cells, elongate smooth with sinuate bodies (20–100 μm long) from long cells, and silica casts of trichomes (10–40 μm long). Hence, the soil phytoliths derived from tree leaves and herbs generally decrease from topsoil to subsoil (Fig. 2a, b; Alexandre et al., 1997; Blecker et al., 2006; Pan et al., 2017).

In *Betula* forest and *Quercus* forest, we concluded that the soil phytoliths were possibly "isometric" and "large" thus resulting in a significantly decreasing content from topsoil to subsoil (Fig. 2a, b). This pattern was supported by previous studies (Alexandre et al., 1997; Blecker et al., 2006; Fishkis et al., 2010; Pan et al., 2017). However, for *Larix* forest (Fig. 2c), the variation in phytolith contents with the different soil layers was not significant. In this forest, herb layer contributed to 40% of the phytoliths while the needles of *Larix principis-rupprechtii* contributed 60% (Table 2), suggesting a mixed contribution of phytoliths in the various soil layers. Considering 95% of the soil phyoliths in *Pinus* forest were predominantly originated from needles of *Pinus tabulaeformis* (Table 2), the increase in the soil phytoliths with depth (0–40 cm) could be attributed to the preferential transport of these phytoliths (Fig. 2d). Sommer et al. (2013) analyzed phytolith distribution and dissolution in forest soils of northern Brandenburg, Germany, and concluded that the dissolution of phytoliths might be one of the main sources for the soil dissolve Si. However, the dissolved phytoliths have not been quantified in present study. Therefore, to better understand the contribution of soil phytoliths to the biogeochemical cycles of Si in our study areas, the quantity of dissolved phytoliths remains to be quantified. Notwithstanding, the soil phytoliths would eventually decrease in deeper soils (Alexandre et al., 1997; Blecker et al., 2006).

Soil characteristics (e.g. bulk density), bioturbation (e.g. earthworm peristalsis) and climatic conditions (e.g. precipitation and temperature) can also affect the distribution and translocation of soil phytoliths (Table 3; Clarke, 2003; Blecker et al., 2006; Fishkis et al., 2009; Zuo et al., 2014). However, these influences were minimal at a small-spatial scale. For instance, there were few earthworm channels and earthworms were found during the soil sampling. In addition, the bulk densities of soil profiles increased slightly with depth across each forest type (Table 3), which implied that the soil phytolith variations caused by soil bulk densities were nearly equivalent among different forests. Therefore, our findings highlight that the community composition, the quantity of phytolith production from each plant species, the biomass ratio of above-ground herbs and tree leaves (or needles), and the origin of soil phytoliths might govern the distribution of soil phytoliths, partly influencing the stability of biogenic silica and the biogeochemical cycles of Si in terrestrial systems.

4.3. Implications for phytolith long-term carbon sequestration in soils

The significant correlation between phytolith content and PhytOC content in vegetation among different forests (Fig. 1b) indicates that increasing phytolith production can promote the potential of phytolith C sequestration. Although most small size phytolith particles (< 2 μm)

with high specific surface area could be quickly dissolved (Meunier et al., 1999; Parr and Sullivan, 2005; Sommer et al., 2013), approximately 80% of phytoliths with relative intact surfaces might be preserved in soils and sediments for 400–3000 years (Meunier et al., 1999; Blecker et al., 2006; Song et al., 2017). Numerous published data based on the extraction of modified microwave digestion showed that the C content in phytoliths varied from 1 g kg^{-1} to > 100 g kg^{-1}, with most studies reporting ranges between 10 g kg^{-1} to 60 g kg^{-1} (Parr et al., 2010; Parr and Sullivan, 2011; Zuo and Lü, 2011; Li et al., 2013, 2013; Song et al., 2017). In present study, the C content in phytoliths was 15.2–54.4 g kg^{-1} among different plant species (Table 1). However, some studies reported that the C content in phytoliths ranged from 1 g kg^{-1} to 5 g kg^{-1} based on the extraction method of rapid H_2SO_4/H_2O_2 digestion (Santos and Alexandre, 2017). The study of Parr and Sullivan (2014) has demonstrated that the procedures of phytoliths can result in the conspicuous difference of C content in phytoliths; and the modified microwave digestion process is more reliable than rapid H_2SO_4/H_2O_2 digestion in quantifying the nature of total C content in phytoliths.

Based on the SEM (scanning electron microscopy) images of phytoliths extracted from microwave digestion and rapid H_2SO_4/H_2O_2 digestion procedures, the C pools in phytoliths could be divided into i) C occluded within cavities of cavate phytoliths and ii) C evenly distributed in both cavate and solid phytoliths (Parr and Sullivan, 2014). Although these two C pools in phytoliths have not been quantified, the second C pool may be more stable than the first one for cavate phytoliths (Parr and Sullivan, 2014; Santos and Alexandre, 2017). In most of natural soils, both pools of PhytOC are protected from dissolution within silica structure at a centennial scale (Song et al., 2016; Zuo et al., 2017). For example, the PhytOC could remain for ~9000 years in ancient paddy soils of Lower Yangtze of southern China (Zuo et al., 2017) and for 363–560 years in soils of broadleaf and conifer forests of northern China (Fig. 4b).

Generally, the annual inputs of foliage and herb are one of the main sources of SOC and PhytOC in terrestrial ecosystems (Vogt, 1991; Dewar and Cannell, 1992; Chen et al., 1997; Feng et al., 1999; Song et al., 2013). Compared with SOC storages, the soil PhytOC storages were obviously lower in *Betula*, *Quercus*, *Larix* and *Pinus* forests (Fig. 4a). However, the turnover time for soil PhytOC was 8–20 times slower than that for SOC (Fig. 4b). It is well established that phytoliths and SOC can migrate to > 200 cm in depth in soil (Alexandre et al., 1997). Thus the migration should be taken in consideration when investigating the accumulation of soil PhytOC and SOC. Therefore as our study was limited to the 0–50 cm soil depth, the storage of SOC and soil PhytOC presented in this study may be underestimated. In addition, the SOC input of different forest soils are also composed of deadwood residues, plant roots and soil microorganisms (Jobbágy and Jackson, 2000; Moritz et al., 2009), which may result in an overestimation of SOC turnover time. In spite of these uncertainties, our results showed that the average ratio of PhytOC/SOC increase from topsoil to the subsoil (Fig. 3). This suggests that most of the SOC would quickly release back to atmosphere at an annual-decadal scale with only a small fraction of the SOC being sequestered in deeper soils; while most of the PhytOC could be accumulated in soils at a centennial-millennial scale due to the protection offered by phytoliths.

5. Conclusions

Phytolith content of 39 sampled plant species varied from 0.65 to 28.2 g kg^{-1}; and the C content in these phytoliths were between 15.2 and 54.4 g kg^{-1}. Our results indicate that the composition of forests plays a crucial role in the quantity of and characteristics of the phytoliths produced and deposited onto soil. This therefore governs the stability and distribution of phytoliths in forest soils. The majority of the phytoliths originated from herbs in the *Betula* and *Quercus* forests, while 95% of the phytoliths originated from *Pinus* needles in the *Pinus* forest. Within the 0–50 cm soil depth, there was 0.29 ± 0.02 t ha^{-1}, 0.67 ± 0.03 t ha^{-1}, 0.46 ± 0.03 t ha^{-1} and 0.37 ± 0.02 t ha^{-1} PhytOC deposited in *Betula*, *Quercus*, *Larix* and *Pinus* forest, respectively. Although soil PhytOC storage was lower than SOC storage, PhytOC is important for the centennial-millennial storage of C, further contributing to long-term C sequestration. Assessing the biogenic Si and its coupled carbon cycles in terrestrial biomes should take into account the influence of ecological community composition.

Acknowledgements

We acknowledge the support from the National Natural Science Foundation of China (41522207, 41571130042) and the State's Key Project of Research and Development Plan of China (2016YFA0601002). We thank Kim McGrouther for her constructive comments and helpful English language editing. We declare no conflict of interest.

Appendix A. Supplementary data

Supplementary data to this article can be found online at https://doi.org/10.1016/j.geoderma.2017.10.005.

References

Alexandre, A., Meunier, J.D., Colin, F., Koud, J.M., 1997. Plant impact on the biogeochemical cycle of silicon and related weathering processes. Geochim. Cosmochim. Acta 61, 677–682.
Bartoli, F., 1983. The biogeochemical cycle of silicon in two temperate forest ecosystems. Environ. Biogeochem. Ecol. Bull. 35, 469–476.
Bartoli, F., 1985. Crystallochemistry and surface properties of biogenic opal. Eur. J. Soil Sci. 36, 335–350.
Bartoli, F., Wilding, L.P., 1980. Dissolution of biogenic opal as a function of its physical and chemical properties. Soil Sci. Soc. Am. J. 44, 873–878.
Blecker, S.W., McCulley, R.L., Chadwick, O.A., Kelly, E.F., 2006. Biologic cycling of silica across a grassland bioclimosequence. Glob. Biogeochem. Cycles 20, GB3023.
Burkhardt, M., Kasteel, R., Vanderborght, J., Vereecken, H., 2008. Field study on colloid transport using fluorescent microspheres. Eur. J. Soil Sci. 59, 82–93.
Carnelli, A.L., Madella, M., Theurillat, J.P., 2001. Biogenic silica production in selected alpine plant species and plant communities. Ann. Bot. 87, 425–434.
Chen, L., Huang, J., Yan, C., 1997. Nutrient Cycles in Forest Ecosystems of China. Meteorology Press of China, Beijing (in Chinese).
Christian, K., 2003. Carbon limitation in trees. J. Ecol. 91, 4–17.
Clarke, J., 2003. The occurrence and significance of biogenic opal in the regolith. Earth Sci. Rev. 60, 175–194.
Colin, F., Brimhall, G.H., Nahon, D., Lewis, C.J., Baronnet, A., Danty, K., 1992. Equatorial rainforest lateritic mantles: a geomembrane filter. Geology 20, 523–526.
Conley, D.J., 2002. Terrestrial ecosystems and the global biogeochemical silica cycle. Glob. Biogeochem. Cycles 16, 1121. http://dx.doi.org/10.1029/2002GB001894.
Cornelis, J.T., Ranger, J., Iserentant, A., Delvaux, B., 2010. Tree species impact the terrestrial cycle of silicon through various uptakes. Biogeochemistry 97, 231–245.
Dewar, R.C., Cannell, M.G.R., 1992. Carbon sequestration in the trees, products and soils of forest plantations: an analysis using UK examples. Tree Physiol. 11, 4–71.
Epstein, E., 1994. The anomaly of silicon in plant biology. P. Natl. Acad. Sci. USA 91, 11–17.
Epstein, E., 2009. Silicon: its manifold roles in plants. Ann. Appl. Biol. 155, 155–160.
Fang, J., Chen, A., Peng, C., Zhao, S., Ci, L., 2001. Changes in forest biomass carbon storage in China between 1949 and 1998. Science 292, 2320–2322.
FAO, 2010. Global Forest Resources Assessment 2010: Main Report. Food and Agriculture Organization of the United Nations, Rome.
Feng, Z., Wang, X., Wu, G., 1999. Biomass and Productivity of Forest Ecosystems in China. Science Press, Beijing (in Chinese).
Fishkis, O., Ingwersen, J., Lamers, M., Denysenko, D., Streck, T., 2010. Phytolith transport in soil: a field study using fluorescent labelling. Geoderma 157, 27–36.
Fishkis, O., Ingwersen, J., Streck, T., 2009. Phytolith transport in sandy sediment: experiments and modeling. Geoderma 151, 168–178.
Fraysse, F., Pokrovsky, O.S., Schott, J., Meunier, J.D., 2009. Surface chemistry and reactivity of plant phytoliths in aqueous solutions. Chem. Geol. 258, 197–206.
Gilliam, F.S., 2007. The ecological significance of the herbaceous layer in temperate forest ecosystems. Bioscience 57, 845–858.
Hodson, M.J., 2016. The development of phytoliths in plants and its influence on their chemistry and isotopic composition. Implications for palaeoecology and archaeology. J. Archaeol. Sci. 68, 62–69.
Hodson, M.J., White, P.J., Mead, A., Broadley, M.R., 2005. Phylogenetic variation in the silicon composition of plants. Ann. Bot. 96, 1027–1046.
IUSS Working Group WRB, 2015. World Reference Base for Soil Resources 2014, Update 2015, International Soil Classification System for Naming Soils and Creating Legends for Soil Maps. World Soil Resources Reports No. 106. FAO, Rome.

Jobbágy, E.G., Jackson, R.B., 2000. The vertical distribution of soil organic carbon and its relation to climate and vegetation. Ecol. Appl. 10, 423–436.
Jones, L.H.P., Milne, A.A., 1963. Studies of silica in the oat plant. Plant Soil 18, 207–220.
Li, Z., Song, Z., Cornelis, J., 2014. Impact of rice cultivar and organ on elemental composition of phytoliths and the release of bio-available silicon. Front. Plant Sci. 5, 529. http://dx.doi.org/10.3389/fpls.2014.00529. (Article 529).
Li, Z., Song, Z., Jiang, P., 2013. Biogeochemical sequestration of carbon within phytoliths of wetland plants: a case study of Xixi wetland, China. Chin. Sci. Bull. 58, 2480–2487.
Li, Z., Song, Z., Parr, J.F., Wang, H., 2013. Occluded C in rice phytoliths: implications to biogeochemical carbon sequestration. Plant Soil 370, 615–623.
Liu, H., Yin, Y., Tian, Y., Ren, J., Wang, H., 2008. Climatic and anthropogenic controls of topsoil features in the semi-arid East Asian steppe. Geophys. Res. Lett. 35. http://dx.doi.org/10.1029/2007GL032980.
Liu, Y., Chen, B., Yang, X., Zhao, X., Wang, Y., 2012. Fractal characteristics of soil particles of typical forest in north mountain of Hebei province. J. Soil Water Conserv. 26, 159–163 (in Chinese with English abstract).
Lu, R., 2000. Methods of Soil and Agrochemical Analysis. China Agricultural Science and Technology Press, Beijing (in Chinese).
Maguire, T.J., Templer, P.H., Battles, J.J., Fulweiler, R.W., 2017. Winter climate change and fine root biogenic silica in sugar maple trees (*Acer saccharum*): implications for silica in the Anthropocene. J. Geophys. Res. Biogeosci. 122, 708–715.
Mawdsley, J.L., Brooks, A.E., Merry, R.J., 1996. Movement of the protozoan pathogen *Cryptosporidium parvum* through three contrasting soil types. Biol. Fertil. Soils 21, 30–36.
Meunier, J.D., Barboni, D., Anwar-ul-Haq, M., Levard, C., Chaurand, P., Vidal, V., Grauby, O., Huc, R., Laffont-Schwob, I., Rabier, J., Keller, C., 2017. Effect of phytoliths for mitigating water stress in durum wheat. New Phytol. 215, 229–239.
Meunier, J.D., Colin, F., Alarcon, C., 1999. Biogenic silica storage in soils. Geology 27, 835–838.
Moritz, L.K., Liang, C., Wagai, R., Kitayama, K., Balser, T.C., 2009. Vertical distribution and pools of microbial residues in tropical forest soils formed from distinct parent materials. Biogeochemistry 92, 83–94.
Pan, W., Song, Z., Liu, H., Van Zwieten, L., Li, Y., Yang, X., Han, Y., Liu, X., Zhang, X., Xu, Z., Wang, H., 2017. The accumulation of phytolith-occluded carbon in soils of different grasslands. J. Soils Sediments 17, 2420–2427. https://doi.org/10.1007/s11368-017-1690-8.
Parr, J.F., Sullivan, L.A., 2005. Soil carbon sequestration in phytoliths. Soil Biol. Biochem. 37, 117–124.
Parr, J.F., Sullivan, L.A., 2011. Phytolith occluded carbon and silica variability in wheat cultivars. Plant Soil 342, 165–171.
Parr, J.F., Sullivan, L.A., 2014. Comparison of two methods for the isolation of phytolith occluded carbon from plant material. Plant Soil 374, 45–53.
Parr, J.F., Sullivan, L.A., Chen, B., Ye, G., Zheng, W., 2010. Carbon bio-sequestration within the phytoliths of economic bamboo species. Glob. Chang. Biol. 16, 2661–2667.
Parr, J.F., Sullivan, L.A., Quirk, R., 2009. Sugarcane phytoliths: encapsulation and sequestration of a long-lived carbon fraction. Sugar Tech. 11, 17–21.
Piperno, D.R., 1985. Phytolith taphonomy and distributions in archeological sediments from Panama. J. Archaeol. Sci. 12, 247–267.
Qiu, S., Liu, H., Zhao, F., Liu, X., 2016. Inconsistent changes of biomass and species richness along a precipitation gradient in temperate steppe. J. Arid Environ. 132, 42–48.
Ricotta, C., Moretti, M., 2011. CWM and Rao's quadratic diversity: a unified framework for functional ecology. Oecologia 167, 181–188.
Rosen, A.M., Weiner, S., 1994. Identifying ancient irrigation: a new method using opaline phytoliths from emmer wheat. J. Archaeol. Sci. 21, 125–132.
Santos, G.M., Alexandre, A., 2017. The phytolith carbon sequestration concept: fact or fiction? A comment on “Occurrence, turnover and carbon sequestration potential of phytoliths in terrestrial ecosystems by song et al.”. Earth Sci. Rev. 164, 251–255. http://dx.doi.org/10.1016/j.earscirev.2016.04.007.
Smith, M.S., Thomas, G.W., White, R.E., Ritonga, D., 1985. Transport of *Erscherichia coli* trough intact and disturbed soil columns. J. Environ. Qual. 14, 87–91.
Sommer, M., Jochheim, H., Höhn, A., Breuer, J., Zagorski, Z., Busse, J., Barkusky, D., Meier, K., Puppe, D., Wanner, M., Kaczorek, D., 2013. Si cycling in a forest biogeosystem—the importance of transient state biogenic Si pools. Biogeosciences 10, 4991–5007.
Song, Z., Liu, H., Li, B., Yang, X., 2013. The production of phytolith-occluded carbon in China's forests: implications to biogeochemical carbon sequestration. Glob. Chang. Biol. 19, 2907–2915.
Song, Z., Liu, H., Si, Y., Yin, Y., 2012. The production of phytoliths in China's grasslands: implications to the biogeochemical sequestration of atmospheric CO_2. Glob. Chang. Biol. 18, 3647–3653.
Song, Z., Liu, H., Strömberg, C.A., Yang, X., Zhang, X., 2017. Phytolith carbon sequestration in global terrestrial biomes. Sci. Total Environ. 603, 502–509.
Song, Z., McGrouther, K., Wang, H., 2016. Occurrence, turnover and carbon sequestration potential of phytoliths in terrestrial ecosystems. Earth Sci. Rev. 158, 19–30.
Song, Z., Wang, H., Strong, P.J., Guo, F., 2014. Phytolith carbon sequestration in China's croplands. Eur. J. Agron. 53, 10–15.
Song, Z., Wang, H., Strong, P.J., Li, Z., Jiang, P., 2012. Plant impact on the coupled terrestrial biogeochemical cycles of silicon and carbon: implications for biogeochemical carbon sequestration. Earth Sci. Rev. 155, 319–331.
Strömberg, C.A.E., 2004. Using phytolith assemblages to reconstruct the origin and spread of grass-dominated habitats in the great plains of North America during the late Eocene to early Miocene. Palaeogeogr. Palaeoclimatol. Palaeoecol. 207, 239–275.
ter Braak, C.J.F., 1986. Canonical correspondence analysis: a new eigenvector technique for multivariate direct gradient analysis. Ecology 67, 1167–1179.
Tian, Y., Qin, F., Yan, H., Guo, W., Guan, Q., 2011. Carbon content rate in the common woody plants of China. J. Anhui Agri. Sci. 39, 16166–16169 (in Chinese with English abstract).
Umemura, M., Takenaka, C., 2014. Biological cycle of silicon in moso bamboo (*Phyllostachys pubescens*) forests in central Japan. Ecol. Res. 29, 501–510.
van Elsas, J.D., Trevors, J.T., van Overbeek, L.S., 1991. Influence of soil properties on the vertical movement of genetically-marked *Pseudomonas fluorescens* through large soil microcosms. Biol. Fertil. Soils 10, 249–255.
Vogt, K., 1991. Carbon budgets of temperate forest ecosystems. Tree Physiol. 9, 69–86.
Walkley, A., Black, I.A., 1934. An examination of the Degtjareff method for determining soil organic matter, and a proposed modification of the chromic acid titration method. Soil Sci. 37, 29–38.
Wang, Y., Lü, H., 1993. Phytolith Study and its Application. China Ocean, Beijing (in Chinese).
Wilding, L.P., 1967. Radiocarbon dating of biogenetic opal. Science 156, 66–67.
Yang, X., Song, Z., Liu, H., Bolan, N.S., Wang, H., Li, Z., 2015. Plant silicon content in forests of north China and its implications for phytolith carbon sequestration. Ecol. Res. 30, 347–355.
Yang, X., Song, Z., Sullivan, L., Wang, H., Li, Z., Li, Y., Zhang, F., 2016. Topographic control on phytolith carbon sequestration in moso bamboo (*Phyllostachys pubescens*) ecosystems. Carbon Manage. 7, 105–112.
Zhang, S., Zhang, J., Slik, J.W., Cao, K., 2012. Leaf element concentrations of terrestrial plants across China are influenced by taxonomy and the environment. Glob. Ecol. Biogeogr. 21, 809–818.
Zhang, W., Yang, X., Zhang, R., Gao, Y., Yao, W., 2011. Evaluation on water conservation functions of litter and soils under different forests in mountainous area of northern Hebei province. B. Soil Water Conserv. 31, 121–208 (in Chinese with English abstract).
Zhao, J., Wang, Y., Yang, X., 2013. Hydrological effects of forest soil in mountain area of northern Hebei. Res. Soil Water Conserv. 20, 201–205 (in Chinese with English abstract).
Zuo, X., Lü, H., 2011. Carbon sequestration within millet phytoliths from dry-farming of crops in China. Chin. Sci. Bull. 56, 3451–3456.
Zuo, X., Lu, H., Gu, Z., 2014. Distribution of soil phytolith-occluded carbon in the Chinese Loess Plateau and its implications for silica–carbon cycles. Plant Soil 374, 223–232.
Zuo, X., Lu, H., Jiang, L., Zhang, J., Yang, X., Huan, X., He, K., Wang, C., Wu, N., 2017. Dating rice remains through phytolith carbon-14 study reveals domestication at the beginning of the Holocene. P. Natl. Acad. Sci. USA 114, 6486–6491.